HHS Public Access

Author manuscript

J Am Acad Child Adolesc Psychiatry. Author manuscript; available in PMC 2016 October 01.

Published in final edited form as:

J Am Acad Child Adolesc Psychiatry. 2015 October ; 54(10): 859–867. doi:10.1016/j.jaac.2015.07.007.

Corticospinal Tract Anatomy and Functional Connectivity of Primary Motor Cortex in Autism

Dr. Ruth A. Carper, PhD,
Brain Development Imaging Laboratory at San Diego State University, CA.

Miss Seraphina Solders [student],
Brain Development Imaging Laboratory at San Diego State University, CA.

Mr. Jeffrey M. Treiber, BA [student of the School of Medicine],
University of California, San Diego.

Dr. Inna Fishman, PhD, and
Brain Development Imaging Laboratory at San Diego State University, CA.

Dr. Ralph-Axel Müller, PhD
Brain Development Imaging Laboratory at San Diego State University, CA.

Abstract

Objective—Growing evidence indicates that autism spectrum disorder (ASD) stems from abnormal structural and functional connectivity of neural networks. While diagnostic symptoms are sociocommunicative, motor-related functions (beyond repetitive mannerisms) are also impaired. However, evidence on connectivity at the level of basic motor execution is limited, which we address here.

Method—We compared right-handed children and adolescents (aged 7-18 years) with ASD (n=44) to matched typically developing participants (TD, n=36) using magnetic resonance imaging (MRI). Diffusion-weighted imaging and probabilistic tractography measured microstructure of the corticospinal tract (CST). Intrinsic functional connectivity MRI examined whole-brain voxel-wise correlations, both with identical precentral gyrus (PCG) seeds.

Results—In the group with ASD, radial and mean diffusivity were increased bilaterally in the CST, particularly in superior segments, and a leftward asymmetry of CST volume detected in the TD group was reversed. Functionally, overconnectivity was found for both left and right PCG with prefrontal, parietal, medial occipital, and cingulate cortices. The group with ASD also showed significantly reduced asymmetry of functional connectivity for both left and right PCG

Correspondence to Ruth Carper, PhD, Brain Development Imaging Laboratory, Department of Psychology, San Diego State University, 6363 Alvarado Ct, Suite 200, San Diego, CA 92120; rcarper99@gmail.com..

Supplemental material cited in this article is available online.

Disclosure: Drs. Carper, Fishman, Müller, Ms. Solders, and Mr. Treiber report no biomedical financial interests or potential conflicts of interest.

seeds. Finally, in the group with ASD, significant correlations were found for functional overconnectivity of the right PCG seed with anisotropy and mean diffusivity in the right CST.

Conclusion—The findings, implicating both functional and anatomical connectivity of primary motor cortex, suggest that network anomalies in ASD go well beyond sociocommunicative domains, affecting basic motor execution. They also suggest that even in right-handed adolescents with ASD, typical left hemisphere dominance is reduced, both anatomically and functionally, with an unusual degree of right hemisphere motor participation.

Keywords

Autism spectrum disorder; diffusion tensor imaging; probabilistic tractography; functional connectivity MRI; primary motor cortex

INTRODUCTION

While autism spectrum disorders (ASD) are diagnosed based on sociocommunicative impairments and restricted or repetitive behaviors,[1] there is increasing evidence that ASD is associated with abnormal motor-related functions beyond repetitive motor mannerisms, including hypotonia,[2] abnormalities of gait,[3,4] and dyspraxia or apraxia.[2] Delays in motor development[5] and impairments of gross and fine motor function[6] have also been reported, and may be present as early as infancy[5,7] and persist into adulthood.[8]

In a typically developing (TD) brain, voluntary movements are controlled by primary motor cortex (M1) and its outputs through the corticospinal tract (CST), with indirect modulation through basal ganglia and cerebellar circuits. Motor abnormalities in ASD are often interpreted as implicating basal ganglia and/or cerebellum,[3,4] whereas evidence related to the motor control system itself remains limited. In 8- to 12-year-olds with ASD, increased white matter volume in the motor/premotor area (precentral gyrus) was found to be predictive of poorer motor function, a reversal of the correlation seen in typical children.[9] The authors suggested that this effect primarily reflected local (rather than long distance) connections. In the present study, we examine connectivity of the motor control system in ASD, including anatomical organization of its output pathway along the CST and functional connectivity of primary motor cortex, using diffusion tensor imaging (DTI) and intrinsic functional connectivity (iFC) magnetic resonance imaging (MRI).

Studies utilizing DTI indicate atypical trajectories for white matter maturation.[10] Toddlers with ASD show increased fractional anisotropy (FA)[11,12] while school-age children and adolescents show reduced FA, increased mean diffusivity (MD), and radial diffusivity (RD). This suggests an early acceleration of maturation followed by a plateau, further supported by longitudinal findings[13] and similar to what is seen in volumetric studies of gray matter.[14-16] Abnormalities have been reported in frontal,[17,18] temporal,[17,18] and parietal white matter,[19] cerebellar peduncles,[20] and large association tracts.[17,21-23] Although none of these studies has systematically examined CST, a few reported limited findings within the tract. Shukla et al.[24] and Jou et al.[21] reported reduced FA and increased MD in segments of the white matter “skeleton” corresponding to CST. One region-of-interest study found decreased FA in

posterior limb of the internal capsule bilaterally and in right inferior CST (cerebral peduncle),[20] while another found increased MD but no effects on FA.[25]

Complementing the investigation of anatomical connectivity through DTI, functional connectivity MRI (fcMRI) assesses functional coordination between spatially distributed brain regions.[26,27] Intrinsic functional connectivity (iFC) – inferred from interregional cross-correlations of the blood oxygen level-dependent (BOLD) signal – can be detected at rest, in the absence of an overt task.[28] Importantly, iFC patterns correspond to brain networks recruited during specific cognitive processes[29,30] and likely reflect functional networks associated with functional specialization.[31,32] The iFC patterns are largely consistent with anatomical connectivity[33,34] and are highly reliable across individuals.[27,33,35]

A growing number of fcMRI studies point to widespread abnormalities in interregional connections in ASD,[26,36,37] including decreased connectivity within a motor system (M1, thalamus, and cerebellum[38]), partially replicated by a study showing reduced iFC between (pre)motor cortex and thalamus.[39] Another study suggested reduced differentiation within M1 between upper and lower limb regions in ASD.[40]

The present study provides a comprehensive and multimodal investigation of anatomical and functional connectivity of the motor control system in children and adolescents with ASD compared to TD children. We used DTI and probabilistic tractography to examine the major output pathway of M1, the CST, and iFC to examine the functional connectivity of M1.

METHOD

Participants

All participants with ASD met *DSM-V* criteria for autism spectrum disorder.[1] Prospective participants with ASD were administered the Autism Diagnostic Observation Schedule (ADOS[41]), and parents were administered the Autism Diagnostic Interview—Revised (ADI-R[42]) with final diagnosis confirmed by an experienced clinical psychologist. Children with known neurological disorders other than ASD (e.g. Fragile X syndrome, epilepsy) were excluded. Prospective TD participants with personal or family history of autism, or personal history of other neurological or psychiatric conditions, were excluded. Additional assessments included the Wechsler Abbreviated Scale of Intelligence (WASI[43]), the Developmental Test of Visual–Motor Integration, 6th Edition (VMI[44]), and the Edinburgh Handedness Inventory.[45] The study was approved by the University of California, San Diego, and San Diego State University institutional review boards, with written informed consent and assent provided by all participants and caregivers.

We scanned 108 children and adolescents, excluding 28 because of: non-right hand preference (4 ASD, 6 TD), exclusionary finding on MRI or other measures (6 ASD, 1 TD), or incomplete or poor-quality data in multiple imaging modalities (8 ASD, 3 TD; additional exclusions for single modalities [DTI or iFC] described in Results; for quality criteria, see “Analysis” sections). The final sample included 44 participants with ASD (8 female) and 36 TD individuals (9 female) aged 7-18 years, all right-handed (Table 1) and matched for age and IQ.

MRI data acquisition

MRI data (GE Discovery MR750 3.0T, 8-channel head coil) included: T1-weighted anatomical scan (fast spoiled gradient echo; TR=8.108; TE=3.172ms; flip angle=8°; resolution=1mm^3); diffusion weighted images (2D echo planar imaging [EPI]; 61 non-collinear diffusion directions at b=1000s/mm^2, one at b=0s/mm^2; TR=8500ms; TE=84.9ms; flip angle=90°; resolution=1.875×1.875×2mm^3); matching field map to correct inhomogeneities (2D GRASS; TR=1097ms; TE=9.5ms; flip angle=45°); functional T2*-weighted EPI (6:10 minute resting-state scan; 185 time points; TR=2000ms; TE=30ms; flip angle=90°; resolution=3.4mm isotropic); matching field map (2D GRASS; TR=614ms; TE=6.5ms; flip angle=45°). Participants viewed a white fixation cross displayed on a black background throughout the resting state scan.

DTI Analysis

Preprocessing used the FMRIB Software Library (FSL, v.5.0[46]) and AFNI (v. 2011_12_21_1014[47]), including correction of field inhomogeneities, resampling to 1×1×1mm^3, removal of non-brain tissue, and eddy current correction. Diffusion tensors, FA, MD, RD, and axial diffusivity (AD) were calculated, and the FA map non-linearly registered to the FMRIB58 FA template. Resulting transformation matrices were inverted and saved to facilitate fiber tracking in native space using standard-space atlases. We assessed all scans for motion through both visual inspection of eddy-corrected data (for signal dropout, image noise, shifts of head placement) and quantification of artifacts.[48-50] Scans with visible evidence of moderate or severe motion were excluded. As our study included children as young as 7 years, we did not exclude scans with mild motion. Motion and related artifacts were then quantified following Yendiki et al.[50] and this motion measure was used as a covariate in all analyses. Mean image translation and rotation applied during eddy correction were recorded, as were severity and frequency of signal dropouts across slices. These quantities were combined into a total motion index (TMI), which has been demonstrated to reduce spurious findings related to motion when used as a nuisance regressor.[50]

Fiber tracking was performed using probabilistic tractography (BEDPOSTX, ProbTrackX[51,52]) in native space. A binary seed mask of precentral gyrus (PCG) was derived from the Harvard-Oxford atlas in standard Montreal Neurological Institute (MNI) space, and a cerebral peduncle target mask was generated manually on the standard brain at z=−18 (see Figure S1, available online) with a stop mask one slice inferior. One thousand streamlines were initiated from each of the ~37,865 seed voxels, giving a probability map of connectivity (0.5-mm step length, curvature threshold=0.2). A minimum threshold for number of streamlines was applied at the 75th percentile (see Figure S2, available online), and the output binarized (see Figure S3, available online). These masks were applied to the DTI maps to obtain mean MD, AD, RD, and FA values for each CST, while mask volumes provided a measure of overall CST size in native space. The CST mask was also separated into three segments along its length based on the ICBM-DTI-81 white-matter labels atlas. These corresponded to (i) inferior CST (−18≤z<−4) lying inferior to the thalamus, (ii) middle CST (−4≤z<19) lying within the internal capsule, adjacent to the thalamus, and (iii) superior CST (z≥19) located within the corona radiata. Total brain volume (TBV), including

all brain parenchyma but excluding CSF, was derived from the eddy-corrected b=0 image using FSL's FAST.

Functional Connectivity Analysis

Functional connectivity processing used AFNI and FSL. The first five frames were discarded resulting in 180 total whole brain volumes. Data were slice-time and motion corrected by realigning to the middle time point, corrected for field inhomogeneity, co-registered to the anatomical image, resampled to 3.0mm isotropic voxels, standardized to the MNI template, and spatially smoothed with an isotropic Gaussian filter to an effective full-width at half-maximum of 6mm, to allow for statistical parametric analysis. Band-pass filtering at $.008<f<.08$ Hz isolated frequencies at which intrinsic network-specific BOLD correlations predominate.[28] Time points with head displacement >1 mm (computed as the root sum of square of displacement between any two time points) and their immediately adjacent time points were censored, as were blocks of time points with <10 usable consecutive images. Mean percentage of data censored from all participants was <1.5%, with no difference between groups (M_{ASD}=1.6%; M_{TD}=1.2%; p=0.81). Nuisance variables for linear trend, 6 rigid-body motion parameters (3 rotational, 3 translational), mean white matter (WM) and ventricular (CSF) signals, and their temporal derivatives (band-pass filtered at $.008<f<.08$ Hz) were modeled and removed with regression. WM and CSF masks were derived by combining FSL's automated tissue segmentation (fsl_anat/FAST) with structural templates of ventricular and subcortical zones and further eroding by one voxel. Finally, the root mean square of displacement (RMSD) across the time series was calculated for each participant and used for group matching.

The average BOLD time course was extracted from left and right PCG using identical seeds, as for probabilistic tractography, but excluding non-gray voxels, and Pearson's correlations were performed with the time courses of all other brain voxels in each participant. Resulting correlation coefficients were Fisher-transformed to *z*-values and entered into one- and two-independent-sample(s) *t*-tests to examine within- and between-group iFC effects. Statistical maps were corrected for multiple comparisons to a cluster-size-corrected threshold of $p<.05$ using Monte Carlo simulation.[53]

RESULTS

Diffusion Tensor Imaging

Eleven participants were excluded from diffusion analyses for excessive motion or other DTI artifacts (6 ASD, 5 TD); another 11 (7 ASD, 4 TD) received an fMRI but not a DTI scan, leaving 31 participants with ASD and 27 TD participants for the following analyses. Groups did not significantly differ in age, IQ, or TMI (see Table S1, available online).

Repeated-measures analyses of covariance (ANCOVAs) were conducted separately on FA, MD, AD, and RD. Cerebral hemisphere was the within-subjects variable, diagnosis the between-subjects variable, and age and TMI were covariates. For analyses of CST volume, TBV was also a covariate to control for individual differences in brain size. CST volume showed a significant interaction between diagnosis and hemisphere but no main effects for

either variable (Table 2). The interaction was due to a shift in asymmetry of CST volume, with TD participants having larger CST volumes in the left hemisphere, but ASD participants showing the reverse. CST volume was significantly related to TMI (p=.046) but not TBV or age. To further examine hemispheric differences, we calculated a volume asymmetry index (AI; [Left−Right/Left+Right]×100), which also differed significantly between groups (F(1,53)=4.04, p=.05; Figure 1A). ANCOVA performed on FA values showed no main effects or interactions, although there was a significant relationship to the age covariate (F(1,54)=14.57, p<.001), with FA increasing with age when collapsing across diagnostic group and hemisphere. There was no significant relationship with TMI. Both RD and MD were significantly higher in ASD than TD. Age was a significant covariate for both tests, with RD (F(1,54)=9.83, p=.003) and MD (F(1,54)=6.54 p=.02) values decreasing with age when collapsing across diagnostic group and hemisphere. There were no significant findings for AD. Effects of age within each diagnostic group are further investigated below.

Given possible confounding effects of motion and the significant relationship found between TMI and CST volume, the above analyses were repeated with tightly motion-matched (p=.9) subgroups of 23 ASD and 25 TD participants. Significant findings were similar (see Table S2, available online).

To better localize group differences along the CST, we separately analyzed superior, middle, and inferior segments (see Table S3, available online). Volume of superior CST (sCST) showed a significant diagnosis-by-hemisphere interaction similar to that for the whole CST (F(1,53)=6.62, p=.01) but no main effects. Significant main effects of group were found for MD (F(1,54)=5.48, p=.02), RD (F(1,54)=6.45, p=.01), and FA (F(1,54)=4.32, p=.04), with MD and RD higher in the group with ASD and FA lower. No significant group differences were found for middle or inferior segments, suggesting that group differences in the main analyses were primarily driven by sCST within the corona radiata.

Reduced FA localized to corona radiata could be a secondary outcome of an increased number of crossing association or thalamo-cortical fibers. To test this, we examined volume fractions of primary (f1) and secondary (f2) fiber components estimated by bedpostX, controlling for age and TMI. Within sCST, f1 was significantly reduced in ASD compared to TD (F(1,54)=5.40, p=.02), but groups did not significantly differ on f2 (F(1,54)=1.91, p=.17), and marginal f2 means were lower in ASD (.106±.003) than TD (.112±.004). Such findings do not support the likelihood of an increased volume of crossing fibers. No main or interaction effects were found for hemisphere.

Functional Connectivity

Eleven participants (8 ASD, 3 TD) were excluded from iFC analyses for missing data or insufficient image quality and 3 participants with ASD were excluded to improve motion matching. Therefore, iFC analyses included 33 ASD and 33 TD participants. Groups did not significantly differ in age, IQ, RMSD, or individual motion parameters (see Table S1, available online).

In both groups, both left and right PCG showed functional connectivity bilaterally with the postcentral, middle cingulate, and inferior and middle temporal gyri, supplementary motor

area, inferior parietal cortex, and portions of dorsolateral prefrontal cortex, as well as putamen, pallidum, thalamus, and cerebellum (Figure 2; details in Table S4, available online). Direct group comparisons revealed several significant clusters of increased connectivity (ASD>TD) for both left and right PCG with the left inferior prefrontal cortex (middle orbital and inferior frontal gyri), bilateral superior and middle frontal gyri, and the left inferior parietal lobule and supramarginal gyrus (see Table S5, available online). Right PCG had additional clusters of overconnectivity with bilateral lingual and pericalcarine gyri, cuneus, precuneus, and bilateral middle cingulate gyrus. A single underconnectivity effect (ASD<TD) was detected for left PCG in the left lateral occipital lobe.

Given hemispheric differences for both iFC and CST volume findings, two asymmetry indices (AIs) were calculated, one for each PCG seed. For each hemisphere, we summed the z' scores across all voxels within significant connectivity clusters (excluding the seed) from the within-group connectivity maps (threshold: $p<1\times10^{-6}$). We applied the formula (L−R/L +R)×100 to those values, with L and R being z' scores from left and right hemispheres, providing separate AIs for left and right PCG seeds. One-way ANCOVA covarying for age showed significantly reduced asymmetry in the group with ASD for both left ($F(1,63)=19.66$, $p<.001$) and right ($F(1,63)=14.96$, $p<.001$) PCG seeds, reflecting greater ipsilateral iFC in the TD group (Figure 1B).

Age effects and Brain-behavior relationships

To examine whether connectivity was related to age, clinical symptoms, or cognitive/ behavioral measures, eight connectivity composite measures were computed to minimize multiple comparisons. For DTI, FA and MD were each averaged across hemispheres since no differences had been found, and AI of CST volume was included given the significant group-by-hemisphere interaction. For iFC, two AIs (for left and right PCG) were included, as well as mean z scores for areas of significant group differences, separate for overconnectivity clusters (observed for left and right PCG) and underconnectivity clusters (left PCG seed only; see Figure 2).

Relationships between age and connectivity were examined for each group. For diffusion measures, partial correlation controlling for TMI showed a significant positive correlation for FA in the group with ASD (r=.550, p=.002), but not the TD group (r=.318, p=.11). Age correlations for other diffusion and for functional measures did not survive correction for multiple comparisons.

The relationship with clinical symptoms was examined for ADOS Communication+Social (CS) total score, ADOS Repetitive Behaviors score, ADI-Social, and ADI-Communication scores (diagnostic algorithm) using Spearman correlations (due to skewed distributions of these clinical measures). We also examined relationships between connectivity composite measures and performance on the VMI, available for 23 ASD and 20 TD participants. The ADI Communication subscore in the group with ASD showed correlations with both bilateral FA (rho=-.388, p=.04) and iFC asymmetry of the left PCG (rho=.434, p=.02), but neither survived correction for multiple comparisons. No other significant correlations were detected for either group.

Cross-modality correlations

Forty-six participants (22 ASD, 24 TD) had high-quality data for both diffusion and iFC analyses (see Table S6, available online). Average z-scores for areas of significant iFC group differences were calculated, again separating overconnectivity and underconnectivity effects for each seed (left, right PCG). Relationships between structural (FA and MD in left and right CST) and functional (average z scores) connectivity were examined with Pearson correlations separately for each group and for PCG seeds in each hemisphere. In the group with ASD, significant correlations were found between iFC overconnectivity of the right PCG seed and FA (r=0.594, p=.004) and MD (r=−.621, p=0.002) of the right CST (Figure 3). No other correlations for either group survived correction for multiple comparisons. iFC asymmetry scores were calculated as described above with no significant correlations between these and DTI asymmetry indices (CST volume, FA, MD) for either group.

DISCUSSION

While sociocommunicative deficits garner most attention in autism research, motor abnormalities are also prominent, including repetitive behaviors, atypical gait,[3,4] and dyspraxia.[2] These deficits are often thought to arise from abnormalities in brain areas that modulate motor behavior, such as cerebellum and basal ganglia,[3,4] whereas imaging evidence implicating the motor execution system itself remains limited.[38,40] Here, we examined both whole brain functional connectivity of the PCG and the anatomical microstructure of the outputs of the motor execution system, namely the CST, using identical seeds.

Anatomical Compromise of CST

The group with ASD showed significantly greater MD and RD in the CST, both in our complete sample and in a tightly motion-matched subsample, suggesting similar structural abnormalities as reported for large association tracts[17,21-23] and other white matter sectors.[17,18,54] Our findings are consistent with previous studies that included part of the CST, using other methods.[21,24] Additionally, we detected reduced FA in superior CST at the level of the corona radiata.

While the cellular basis of group differences cannot be conclusively determined from tensor measures, possibilities include differences of myelination, axon caliber, intra-axonal structure, or presence of crossing fibers.[55] However, the volume fraction of the secondary fiber compartment (f2) was not increased, arguing against an increase in crossing fibers, while differences in radial – but not axial – diffusivity suggest reduced myelination,[56-58] or reduced axon number or packing density.[59] Reduced number or packing density (and reduced FA) would be most evident in superior CST, where tightly packed axons begin to fan to reach the expanse of M1, as indeed observed here. Both reduced myelination and reduced axonal number could result from reduced CST activity, given known effects of neural activity on myelination and cell survival.[60,61]

In the TD brain, FA increases as tracts mature, with connections to unimodal areas peaking earlier than those to multimodal areas.[62-64] FA changes in CST are not always detected in

adolescence, possibly due to an asymptote earlier in childhood.[62,63] As seen in our partial-correlation analyses, age-related FA increase was non-significant in our TD group but robust and significant in our group with ASD, possibly reflecting delayed but ongoing motor maturation.

A further finding in ASD was atypical asymmetry. Our TD group showed larger CST volumes in the dominant left hemisphere than the right, similar to typical right-handed adults,[65] but asymmetry was absent or reversed in ASD, although all participants were right-handed. Although absolute measures of tract volume can be affected by image quality, relative volumes and asymmetry ratios, such as those used here, should be more stable and reliable. Additionally, rightward shifts of structural[66-68] and functional[69-71] asymmetry are common findings in language areas in ASD, including rightward shifts for receptive language as early as 12 months of age.[72] A recent iFC study[73] showed rightward asymmetry shifts in numerous sensorimotor, visuospatial, frontal-executive, and frontoparietal networks, suggesting that atypical functional asymmetry may be pervasive in ASD.

Cortical Functional Overconnectivity of M1

Functional connectivity analyses identified overconnectivity clusters in ASD for both left and right PCG seeds including in frontal and parietal association areas. Right PCG was also overconnected with bilateral calcarine cortex, cuneus, and bilateral middle cingulate gyrus. This atypical connectivity between primary motor and primary visual cortices may relate to a general increase in visual activity in ASD, as identified in a meta-analysis,[74] and to fcMRI findings of increased occipito-frontal connectivity.[75,76]

M1 was predominantly overconnected with brain regions outside the motor network proper, as seen in the TD group, suggesting reduced functional segregation of the motor execution system in children with ASD. By contrast, typical development is characterized by increasing network integration (strengthening connections within neurotypical networks) and segregation.[32,77-79] This typical trajectory of network maturation appears disrupted in ASD. Increased M1 iFC observed here is thus in line with recent evidence of reduced or delayed network segregation (or differentiation) in ASD,[40,80-82] possibly due to impaired synaptic pruning.[83] Findings add to growing evidence[80,82,84,85] incompatible with the theory of generally reduced long-distance connectivity in ASD[86,87] or the more specific hypothesis of frontoparietal underconnectivity.[37]

Functional overconnectivity in the ASD group was more pronounced for right than left PCG and was correlated with white matter microstructure of right CST. This suggests that right PCG overconnectivity is an aspect of pervasive shifts in structural and functional asymmetry, discussed above. Functional asymmetry of unilateral PCG seeds also differed, being predominantly ipsilateral in the TD group, whereas in the group with ASD, functional connectivity with contralateral regions was atypically strengthened. Thus, both functional and structural connectivity were atypical in ASD with the most prominent differences related to asymmetry.

Our multimodal analyses benefited from complementary strengths of DTI and iFC to examine different components of the motor execution system. DTI analyses examined the

output tract of PCG, but although cortical seeds were identical for iFC, no directly corresponding analysis was possible. Instead, iFC was well suited to examine cortical connections. Despite unavoidable differences, both analyses tapped into the motor execution system, as reflected in correlations detected between our iFC and DTI findings.

Although the core symptoms of ASD lie in the sociocommunicative domain, our findings show that systems supporting motor execution are affected with respect to both functional and anatomical connectivity. Remarkably, children with ASD showed both white matter compromise, particularly in superior CST, and predominant functional overconnectivity of primary motor cortex, suggesting reduced differentiation of motor execution networks. Finally, our findings add to growing evidence of atypical asymmetries in ASD. These appear to reflect general and potentially pervasive anomalies of cerebral lateralization.

Supplementary Material

Refer to Web version on PubMed Central for supplementary material.

Acknowledgments

This study was supported by the National Institutes of Health R01-MH081023 and K01-MH097972.

The authors specially thank the children and families who participated in the study.

References

1. American Psychiatric Association. Diagnostic and Statistical Manual of Mental Disorders. 5th ed.. American Psychiatric Association; Washington, DC: 2013.
2. Ming X, Brimacombe M, Wagner GC. Prevalence of motor impairment in autism spectrum disorders. Brain Dev. 2007; 29:565–570. [PubMed: 17467940]
3. Esposito G, Venuti P, Apicella F, Muratori F. Analysis of unsupported gait in toddlers with autism. Brain Dev. 2011; 33:367–373. [PubMed: 20708861]
4. Nayate A, Tonge BJ, Bradshaw JL, Mcginley JL, Iansek R, Rinehart NJ. Differentiation of high-functioning autism and Asperger's disorder based on neuromotor behaviour. J Autism Dev Disord. 2012; 42:707–717. [PubMed: 21660499]
5. Ozonoff S, Young GS, Goldring S, et al. Gross motor development, movement abnormalities, and early identification of autism. J Autism Dev Disord. 2008; 38:644–656. [PubMed: 17805956]
6. Provost B, Lopez BR, Heimerl S. A comparison of motor delays in young children: autism spectrum disorder, developmental delay, and developmental concerns. J Autism Dev Disord. 2007; 37:321–328. [PubMed: 16868847]
7. Teitelbaum P, Teitelbaum O, Nye J, Fryman J, Maurer RG. Movement analysis in infancy may be useful for early diagnosis of autism. Proceedings of the National Academy of Sciences of the United States of America. 1998; 95:13982–13987. [PubMed: 9811912]
8. Fournier KA, Hass CJ, Naik SK, Lodha N, Cauraugh JH. Motor coordination in autism spectrum disorders: a synthesis and meta-analysis. J Autism Dev Disord. 2010; 40:1227–1240. [PubMed: 20195737]
9. Mostofsky SH, Burgess MP, Gidley Larson JC. Increased motor cortex white matter volume predicts motor impairment in autism. Brain. 2007; 130:2117–2122. [PubMed: 17575280]
10. Travers BG, Adluru N, Ennis C, et al. Diffusion Tensor Imaging in Autism Spectrum Disorder: A Review. Autism Res. 2012; 5:289–313. [PubMed: 22786754]
11. Ben Bashat D, Kronfeld-Duenias V, Zachor DA, et al. Accelerated maturation of white matter in young children with autism: a high b value DWI study. NeuroImage. 2007; 37:40–47. [PubMed: 17566764]

12. Weinstein M, Ben-Sira L, Levy Y, et al. Abnormal white matter integrity in young children with autism. Hum. Brain Mapp. 2010; 32:534–543. [PubMed: 21391246]
13. Wolff JJ, Gu H, Gerig G, et al. Differences in white matter fiber tract development present from 6 to 24 months in infants with autism. The American journal of psychiatry. 2012; 169:589–600. [PubMed: 22362397]
14. Carper RA, Moses P, Tigue ZD, Courchesne E. Cerebral lobes in autism: Early hyperplasia and abnormal age effects. NeuroImage. 2002; 16:1038–1051. [PubMed: 12202091]
15. Hazlett HC, Poe MD, Gerig G, et al. Early brain overgrowth in autism associated with an increase in cortical surface area before age 2 years. Arch Gen Psychiatry. 2011; 68:467–476. [PubMed: 21536976]
16. Zielinski BA, Prigge MBD, Nielsen JA, et al. Longitudinal changes in cortical thickness in autism and typical development. Brain. 2014; 137:1799–1812. [PubMed: 24755274]
17. Noriuchi M, Kikuchi Y, Yoshiura T, et al. Altered white matter fractional anisotropy and social impairment in children with autism spectrum disorder. Brain Res. 2010; 1362:141–149. [PubMed: 20858472]
18. Cheung C, Chua SE, Cheung V, et al. White matter fractional anisotrophy differences and correlates of diagnostic symptoms in autism. Journal of child psychology and psychiatry, and allied disciplines. 2009; 50:1102–1112.
19. Shukla DK, Keehn B, Smylie DM, Müller R-A. Microstructural abnormalities of short-distance white matter tracts in autism spectrum disorder. Neuropsychologia. 2011; 49:1378–1382. [PubMed: 21333661]
20. Brito AR, Vasconcelos MM, Domingues RC, et al. Diffusion tensor imaging findings in school-aged autistic children. J Neuroimaging. 2009; 19:337–343. [PubMed: 19490374]
21. Jou RJ, Mateljevic N, Kaiser MD, Sugrue DR, Volkmar FR, Pelphrey KA. Structural neural phenotype of autism: preliminary evidence from a diffusion tensor imaging study using tract-based spatial statistics. AJNR Am J Neuroradiol. 2011; 32:1607–1613. [PubMed: 21799040]
22. Bode MK, Mattila M-L, Kiviniemi V, et al. White matter in autism spectrum disorders - evidence of impaired fiber formation. Acta Radiol. 2011; 52:1169–1174. [PubMed: 22101385]
23. Fletcher PT, Whitaker RT, Tao R, et al. Microstructural connectivity of the arcuate fasciculus in adolescents with high-functioning autism. NeuroImage. 2010; 51:1117–1125. [PubMed: 20132894]
24. Shukla DK, Keehn B, Müller R-A. Tract-specific analyses of diffusion tensor imaging show widespread white matter compromise in autism spectrum disorder. Journal of child psychology and psychiatry, and allied disciplines. 2010; 52:286–295.
25. Pryweller JR, Schauder KB, Anderson AW, et al. White matter correlates of sensory processing in autism spectrum disorders. Neuroimage Clin. 2014; 6:379–387. [PubMed: 25379451]
26. Vissers ME, Cohen MX, Geurts HM. Brain connectivity and high functioning autism: a promising path of research that needs refined models, methodological convergence, and stronger behavioral links. Neurosci. Biobehav. Rev. 2012; 36:604–625. [PubMed: 21963441]
27. Van Dijk KR, Hedden T, Venkataraman A, Evans KC, Lazar SW, Buckner RL. Intrinsic functional connectivity as a tool for human connectomics: theory, properties, and optimization. J Neurophysiol. 2010; 103:297–321. [PubMed: 19889849]
28. Fox MD, Raichle ME. Spontaneous fluctuations in brain activity observed with functional magnetic resonance imaging. Nat Rev Neurosci. 2007; 8:700–711. [PubMed: 17704812]
29. Allen EA, Erhardt EB, Damaraju E, et al. A baseline for the multivariate comparison of resting-state networks. Front Syst Neurosci. 2011; 5:2. [PubMed: 21442040]
30. Smith SM, Fox PT, Miller KL, et al. Correspondence of the brain's functional architecture during activation and rest. Proc Natl Acad Sci USA. 2009; 106:13040–13045. [PubMed: 19620724]
31. Fair DA, Dosenbach NUF, Church JA, et al. Development of distinct control networks through segregation and integration. Proc Natl Acad Sci USA. 2007; 104:13507–13512. [PubMed: 17679691]
32. Fair DA, Cohen AL, Power JD, et al. Functional brain networks develop from a “local to distributed” organization. PLoS Comput Biol. 2009; 5:e1000381. [PubMed: 19412534]

33. Honey CJ, Sporns O, Cammoun L, et al. Predicting human resting-state functional connectivity from structural connectivity. Proc Natl Acad Sci USA. 2009; 106:2035–2040. [PubMed: 19188601]
34. Greicius MD, Supekar K, Menon V, Dougherty RF. Resting-state functional connectivity reflects structural connectivity in the default mode network. Cereb Cortex. 2009; 19:72–78. [PubMed: 18403396]
35. Damoiseaux JS, Rombouts SARB, Barkhof F, et al. Consistent resting-state networks across healthy subjects. Proc Natl Acad Sci USA. 2006; 103:13848–13853. [PubMed: 16945915]
36. Müller R-A. The study of autism as a distributed disorder. Mental retardation and developmental disabilities research reviews. 2007; 13:85–95. [PubMed: 17326118]
37. Schipul SE, Keller TA, Just MA. Inter-regional brain communication and its disturbance in autism. Front Syst Neurosci. 2011; 5:10. [PubMed: 21390284]
38. Mostofsky SH, Powell SK, Simmonds DJ, Goldberg MC, Caffo B, Pekar JJ. Decreased connectivity and cerebellar activity in autism during motor task performance. Brain. 2009; 132:2413–2425. [PubMed: 19389870]
39. Nair A, Treiber JM, Shukla DK, Shih P, Müller R-A. Impaired thalamocortical connectivity in autism spectrum disorder: a study of functional and anatomical connectivity. Brain. 2013; 136:1942–1955. [PubMed: 23739917]
40. Nebel MB, Joel SE, Muschelli J, et al. Disruption of functional organization within the primary motor cortex in children with autism. Hum Brain Mapp. 2014; 35:567–580. [PubMed: 23118015]
41. Lord, C.; Rutter, M.; DiLavore, P.; Risi, S. Autism Diagnostic Observation Schedule. Western Psychological Services; Los Angeles, CA: 2001.
42. Rutter, M.; Lord, C.; LeCouteur, A. Autism Diagnostic Interview - Revised. Department of Psychiatry, University of Chicago; Chicago: 1995.
43. Wechsler, D. Wechsler Abbreviated Scale of Intelligence. Psychological Corporation; San Antonio, TX: 1999.
44. Beery, K.; Butenica, NA.; Beery, NA. The Beery-Buktenica Developmental Test of Visual-Motor Integration. 6th Edition. Modern Curriculum Press; Parsippany, NJ: 2010.
45. Oldfield RC. The assessment and analysis of handedness: the Edinburgh inventory. Neuropsychologia. 1971; 9:97–113. [PubMed: 5146491]
46. Smith SM, Jenkinson M, Woolrich MW, et al. Advances in functional and structural MR image analysis and implementation as FSL. NeuroImage. 2004; 23(Suppl 1):S208–219. [PubMed: 15501092]
47. Cox RW. AFNI: software for analysis and visualization of functional magnetic resonance neuroimages. Comput Biomed Res. 1996; 29:162–173. [PubMed: 8812068]
48. Koldewyn K, Yendiki A, Weigelt S, et al. Differences in the right inferior longitudinal fasciculus but no general disruption of white matter tracts in children with autism spectrum disorder. Proc Natl Acad Sci USA. 2014; 111:1981–1986. [PubMed: 24449864]
49. Ling J, Merideth F, Caprihan A, Pena A, Teshiba T, Mayer AR. Head injury or head motion? Assessment and quantification of motion artifacts in diffusion tensor imaging studies. Hum Brain Mapp. 2012; 33:50–62. [PubMed: 21391258]
50. Yendiki A, Koldewyn K, Kakunoori S, Kanwisher N, Fischl B. Spurious group differences due to head motion in a diffusion MRI study. NeuroImage. 2013; 88C:79–90. [PubMed: 24269273]
51. Behrens TE, Woolrich MW, Jenkinson M, et al. Characterization and propagation of uncertainty in diffusion-weighted MR imaging. Magn Reson Med. 2003; 50:1077–1088. [PubMed: 14587019]
52. Behrens TEJ, Johansen-Berg H, Jbabdi S, Rushworth MFS, Woolrich MW. Probabilistic diffusion tractography with multiple fibre orientations: What can we gain? NeuroImage. 2007; 34:144–155. [PubMed: 17070705]
53. Forman SD, Cohen JD, Fitzgerald M, Eddy WF, Mintun MA, Noll DC. Improved assessment of significant activation in functional magnetic resonance imaging (fMRI): use of a cluster-size threshold. Magn Reson Med. 1995; 33:636–647. [PubMed: 7596267]
54. Thakkar KN, Polli FE, Joseph RM, et al. Response monitoring, repetitive behaviour and anterior cingulate abnormalities in autism spectrum disorders (ASD). Brain. 2008; 131:2464–2478. [PubMed: 18550622]

55. Beaulieu C. The basis of anisotropic water diffusion in the nervous system - a technical review. NMR in biomedicine. 2002; 15:435–455. [PubMed: 12489094]
56. Harsan LA, Poulet P, Guignard B, et al. Brain dysmyelination and recovery assessment by noninvasive in vivo diffusion tensor magnetic resonance imaging. J Neurosci Res. 2006; 83:392–402. [PubMed: 16397901]
57. Kozlowski P, Raj D, Liu J, Lam C, Yung AC, Tetzlaff W. Characterizing white matter damage in rat spinal cord with quantitative MRI and histology. J Neurotrauma. 2008; 25:653–676. [PubMed: 18578635]
58. Song S-K, Sun S-W, Ramsbottom MJ, Chang C, Russell J, Cross AH. Dysmyelination revealed through MRI as increased radial (but unchanged axial) diffusion of water. NeuroImage. 2002; 17:1429–1436. [PubMed: 12414282]
59. Schwartz ED, Cooper ET, Fan Y, et al. MRI diffusion coefficients in spinal cord correlate with axon morphometry. NeuroReport. 2005; 16:73–76. [PubMed: 15618894]
60. Ishibashi T, Dakin KA, Stevens B, et al. Astrocytes promote myelination in response to electrical impulses. Neuron. 2006; 49:823–832. [PubMed: 16543131]
61. Stevens B, Porta S, Haak LL, Gallo V, Fields RD. Adenosine: a neuron-glial transmitter promoting myelination in the CNS in response to action potentials. Neuron. 2002; 36:855–868. [PubMed: 12467589]
62. Gao W, Lin W, Chen Y, et al. Temporal and spatial development of axonal maturation and myelination of white matter in the developing brain. AJNR Am J Neuroradiol. 2009; 30:290–296. [PubMed: 19001533]
63. Kochunov P, Williamson DE, Lancaster J, et al. Fractional anisotropy of water diffusion in cerebral white matter across the lifespan. Neurobiology of Aging. 2012; 33:9–20. [PubMed: 20122755]
64. Lebel C, Walker L, Leemans A, Phillips L, Beaulieu C. Microstructural maturation of the human brain from childhood to adulthood. NeuroImage. 2008; 40:1044–1055. [PubMed: 18295509]
65. Thiebaut de Schotten M, Ffytche DH, Bizzi A, et al. Atlasing location, asymmetry and inter-subject variability of white matter tracts in the human brain with MR diffusion tractography. NeuroImage. 2011; 54:49–59. [PubMed: 20682348]
66. De Fosse L, Hodge SM, Makris N, et al. Language-association cortex asymmetry in autism and specific language impairment. Ann Neurol. 2004; 56:757–766. [PubMed: 15478219]
67. Lo Y-C, Soong W-T, Gau SS-F, et al. The loss of asymmetry and reduced interhemispheric connectivity in adolescents with autism: A study using diffusion spectrum imaging tractography. Psychiatry Research: Neuroimaging. 2011; 192:60–66. [PubMed: 21377337]
68. Knaus TA, Silver AM, Kennedy M, et al. Language laterality in autism spectrum disorder and typical controls: a functional, volumetric, and diffusion tensor MRI study. Brain Lang. 2010; 112:113–120. [PubMed: 20031197]
69. Kleinhans NM, Müller R-A, Cohen DN, Courchesne E. Atypical functional lateralization of language in autism spectrum disorders. Brain Res. 2008; 1221:115–125. [PubMed: 18555209]
70. Dawson G, Warrenburg S, Fuller P. Hemisphere functioning and motor imitation in autistic persons. Brain Cogn. 1983; 2:346–354. [PubMed: 6546031]
71. Flagg EJ, Cardy JEO, Roberts W, Roberts TPL. Language lateralization development in children with autism: insights from the late field magnetoencephalogram. Neurosci Lett. 2005; 386:82–87. [PubMed: 16046066]
72. Eyler LT, Pierce K, Courchesne E. A failure of left temporal cortex to specialize for language is an early emerging and fundamental property of autism. Brain. 2012; 135:949–960. [PubMed: 22350062]
73. Cardinale RC, Shih P, Fishman I, Ford LM, Müller R-A. Pervasive rightward asymmetry shifts of functional networks in Autism Spectrum Disorder. JAMA Psychiatry. 2013; 70:975–982. [PubMed: 23903586]
74. Samson F, Mottron L, Soulières I, Zeffiro TA. Enhanced visual functioning in autism: an ALE meta-analysis. Hum Brain Mapp. 2012; 33:1553–1581. [PubMed: 21465627]

75. Keehn B, Shih P, Brenner L, Townsend J, Müller R-A. Functional connectivity for an “island of sparing” in autism spectrum disorder: An fMRI study of visual search. Human Brain Mapping. 2013; 34:2524–2537. [PubMed: 22495745]

76. Noonan SK, Haist F, Müller R-A. Aberrant functional connectivity in autism: Evidence from low-frequency BOLD signal fluctuations. Brain Research. 2009; 1262:48–63. [PubMed: 19401185]

77. Dosenbach NU, Nardos B, Cohen AL, et al. Prediction of individual brain maturity using fMRI. Science. 2010; 329:1358–1361. [PubMed: 20829489]

78. Supekar K, Musen M, Menon V. Development of large-scale functional brain networks in children. PLoS Biol. 2009; 7:e1000157. [PubMed: 19621066]

79. Johnson MH. Interactive specialization: A domain-general framework for human functional brain development. Developmental Cognitive Neuroscience. 2011; 1:7–21. [PubMed: 22436416]

80. Fishman I, Keown CL, Lincoln AJ, Pineda JA, Müller R-A. Atypical Cross Talk Between Mentalizing and Mirror Neuron Networks in Autism Spectrum Disorder. JAMA Psychiatry. 2014; 71:751–760. [PubMed: 24740586]

81. Rudie JD, Brown JA, Beck-Pancer D, et al. Altered functional and structural brain network organization in autism. Neuroimage: Clinical. 2013; 2:79–94. [PubMed: 24179761]

82. Shih P, Keehn B, Oram JK, Leyden KM, Keown CL, Müller R-A. Functional differentiation of posterior superior temporal sulcus in autism: A functional connectivity magnetic resonance imaging study. Biological Psychiatry. 2011; 70:270–277. [PubMed: 21601832]

83. Tang G, Gudsnuk K, Kuo SH, et al. Loss of mTOR-Dependent Macroautophagy Causes Autistic-like Synaptic Pruning Deficits. Neuron. 2014; 83:1131–1143. [PubMed: 25155956]

84. Di Martino A, Kelly C, Grzadzinski R, et al. Aberrant striatal functional connectivity in children with autism. Biol Psychiatry. 2011; 69:847–856. [PubMed: 21195388]

85. Rudie JD, Dapretto M. Convergent evidence of brain overconnectivity in children with autism? Cell Rep. 2013; 5:565–566. [PubMed: 24238089]

86. Just MA, Cherkassky VL, Keller TA, Minshew NJ. Cortical activation and synchronization during sentence comprehension in high-functioning autism: evidence of underconnectivity. Brain. 2004; 127:1811–1821. [PubMed: 15215213]

87. Kana RK, Keller TA, Minshew NJ, Just MA. Inhibitory control in high-functioning autism: decreased activation and underconnectivity in inhibition networks. Biol Psychiatry. 2007; 62:198–206. [PubMed: 17137558]

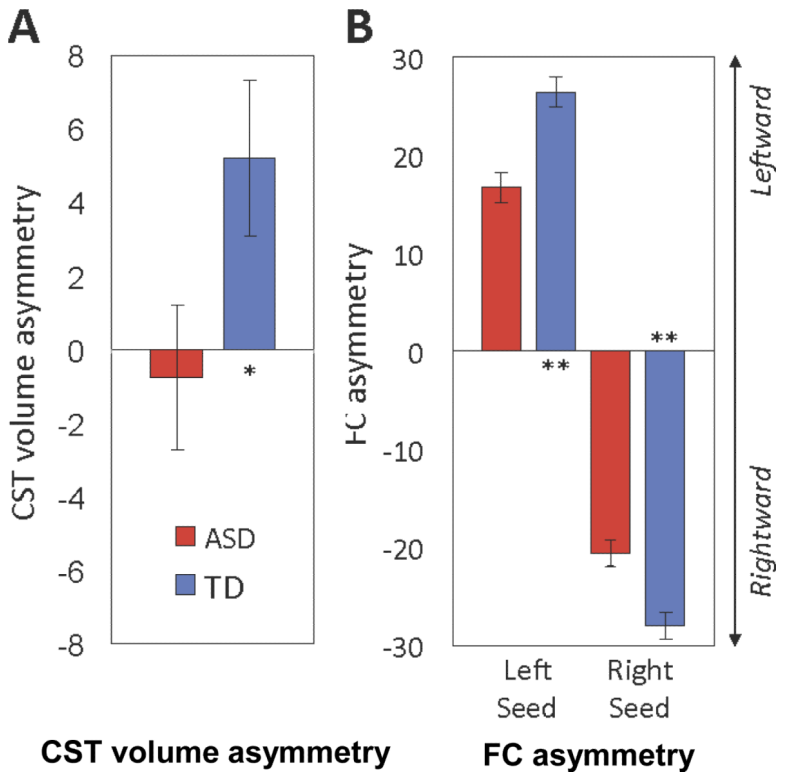

Figure 1.

A. Leftward asymmetry of corticospinal tract (CST) volume observed in the typically developing (TD) group is significantly reduced in the group with autism spectrum disorders (ASD). Note: Bar graphs show marginal means ±1 standard error of the mean after covarying for age, total motion index, and total brain volume. B. Both the left and right precentral gyrus seeds show significant reductions in asymmetry of functional connectivity in the ASD compared to the TD group. In both panels, leftward asymmetry is up (positive values on y axis); rightward asymmetry is down (negative values). *p<.05; **p<.001.

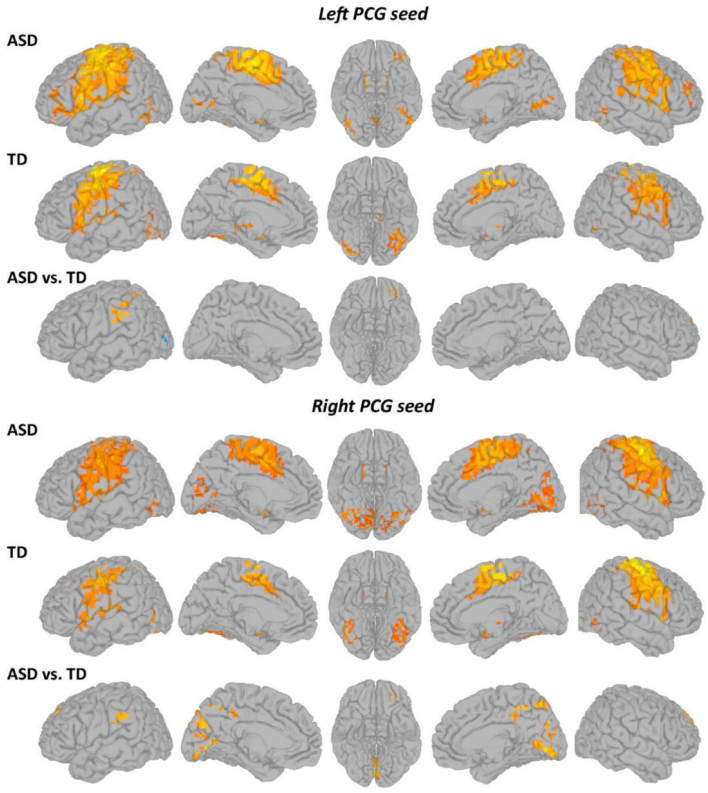

Figure 2.

Within- ($p<1\times10^{-6}$, corr.) and between-group ($p<.05$, corr.) statistical maps of functional connectivity of the left and right precentral gyri (PCG; warm colors represent greater connectivity). Note: ASD = autism spectrum disorder; TD = typically developing.

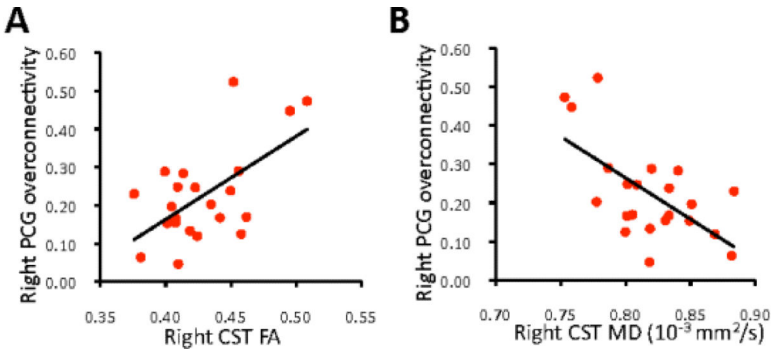

Figure 3.

Functional overconnectivity of right precentral gyrus (PCG) in autism spectrum disorders (average z-scores derived from all significant clusters showing overconnectivity effects) is (A) correlated with fractional anisotropy (FA; r=0.594, *p*=.004) and (B) inversely correlated with mean diffusion (MD; r= −.621, *p*=.002) of the corticospinal tract (CST; n=22).

Table 1

Participant Demographics

	ASD[a] (n=44, 8 female) mean ± SD; range	TD[b] (n=36, 9 female) mean ± SD; range	*p*-value
Age (years)	13.2±2.9; 7-18	12.8±2.4; 8-17	.50
Nonverbal IQ	104.5±17.9; 69-140	105.4±11.8; 83-129	.79
Verbal IQ	100.7±20.4; 56-147	106.1±12.4; 73-133	.17
Full-Scale IQ	102.4±18.7; 66-141	106.5±11.9; 79-132	.26
SRS Total	79.7±10.4; 57-100	41.9±5.0; 35-52	<.001
ADOS Social	9.0±3.5; 4-21		
ADOS Communication	4.3±2.5; 0-13		
ADOS S+C	12.6±4.9; 1-22		
ADOS Repetitive Behavior	2.2±1.6; 0-6		
ADI Social	19.1±5.9; 6-28		
ADI Communication	15.2±5.9; 2-25		
ADI Repetitive Behavior	6.5±2.3; 3-12		
DTI Total Motion Index (TMI)	2.61±4.71; −1.50-18.70	0.87±2.53; −1.97-10.88	0.07
iFC-MRI RMSD	0.10±0.07; 0.02-0.30	0.09±0.07; 0.02-0.30	0.46

Note: ADI-R = Autism Diagnostic Interview-Revised; ADOS = Autism Diagnostic Observation Schedule; DTI = diffusion tensor imaging; iFC-MRI = intrinsic functional connectivity magnetic resonance imaging; RMSD = root mean square of displacement; S+C = Social+Communication subscale; SRS = Social Responsiveness Scale; TD = typically developing.

[a] IQ scores unavailable for 2 participants; SRS unavailable for 1 participant; ADOS scores unavailable for 4 participants; ADI-R scores unavailable for 2 participants.

[b] SRS scores unavailable for 2 participants.

Table 2

Diffusion Measures in Corticospinal Tract

	ASD (n=31)		TD (n=27)		ANCOVA group comparison		ANCOVA group × hemisphere	
	Mean	**SD**	**Mean**	**SD**	***F***	***p***	***F***	***p***
TBV (cm^3)	1271.95	105.82	1225.18	88.35	3.37	.07	---	---
CST Volume (cm^3)								
Left	28.60	7.32	30.41	8.43	0.02	.90	4.52	.04
Right	29.05	8.49	28.24	8.68				
FA								
Left	0.4249	0.0246	0.4322	0.0187	3.47	.07	0.97	.33
Right	0.4259	0.0335	0.4396	0.0234				
MD (10^{-3} mm^2/s)								
Left	0.8183	0.0356	0.8012	0.0228	5.33	.03	0.00	1.00
Right	0.8161	0.0326	0.8015	0.0282				
AD (10^{-3} mm^2/s)								
Left	1.2103	0.0347	1.1962	0.0339	1.04	.31	1.00	.32
Right	1.2065	0.0319	1.2027	0.0378				
RD (10^{-3} mm^2/s)								
Left	0.6223	0.0403	0.6037	0.0237	6.34	.02	0.11	.74
Right	0.6210	0.0417	0.6009	0.0307				

Note: AD = axial diffusivity; ANCOVA = analysis of covariance; ASD = autism spectrum disorders; CST = corticospinal tract; FA = fractional anisotropy; MD = mean diffusivity; RD = radial diffusivity; TBV = total brain volume; TD = typically developing.